# Direct Synthesis of Artificial Esterase through Molecular Imprinting Using a Substrate-Mimicking Acylthiourea Template

Mohan Lakavathu and Yan Zhao\*

Department of Chemistry, Iowa State University, Ames, Iowa 50011-3111, USA

**ABSTRACT:** Most reported artificial esterases only hydrolyze activated esters. We here report a one-pot synthesis of artificial esterases via molecular imprinting. An acylthiourea template hydrogen bonds with 4-vinylbenzoic acid and coordinates to a polymerizable zinc complex inside a cross-linkable surfactant micelle. Double cross-linking of the micelle yields a polymeric nanoparticle catalyst that mimics a metalloenzyme to activate a water molecule for nucleophilic attack on the bound ester. The catalyst hydrolyzes both activated and unactivated esters under mild conditions with selectivity.

**KEYWORDS:** artificial enzyme, molecular imprinting, active site, cooperative catalysis, ester hydrolysis

Ester is a functional group found in numerous natural and manmade products in huge quantities—e.g., fats, oils, and polyesters. Transformation of this functional group is important to diverse fields including soap making, biodiesel production, and polymer recycling. Hydrolysis of esters is slow at neutral pH under ambient conditions. The textbook strategy to speed up the reaction is to activate the carbonyl using an acid catalyst or to employ a more nucleophilic hydroxide to attack the carbonyl. The latter is particularly powerful, as the secondary rate constant for ester hydrolysis by hydroxide is  $10^{7-11}$  times faster than that by water.<sup>1</sup>

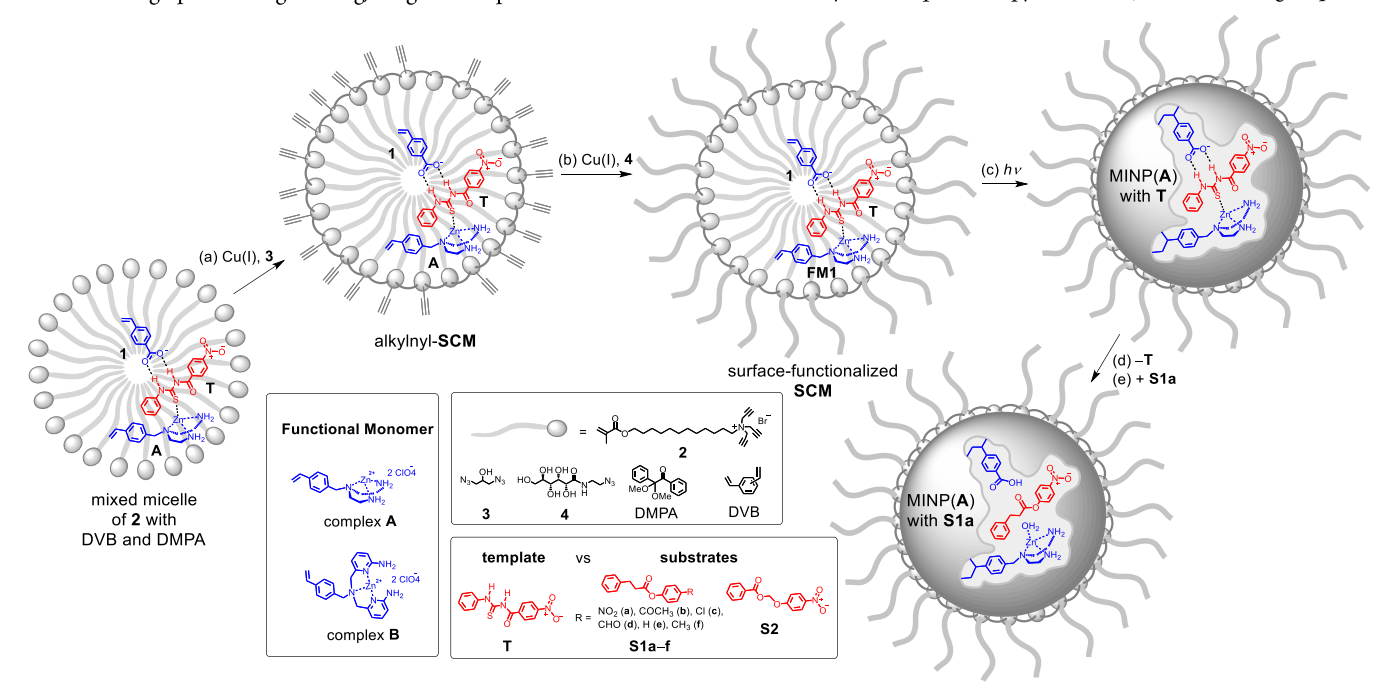
Natural enzymes (esterases) employ similar strategies to hydrolyze esters even though strongly acidic or basic conditions are not available. Many esterases activate an active site serine<sup>2</sup> or water molecule<sup>3</sup> by a nearby histidine, turning them into strong nucleophiles equivalent to alkoxide or hydroxide, respectively. With additional groups to stabilize the tetrahedral intermediate, these enzymes easily hydrolyze unactivated esters under physiological conditions.

Chemists have long been interested in duplicating the catalysis of esterases in synthetic catalysts,<sup>4-7</sup> including those prepared through molecular imprinting.<sup>8-13</sup> In recent years, researchers continue to explore new ways to build artificial esterases.<sup>14-23</sup> and improve natural esterases through protein engineering.<sup>24-26</sup> given the prevalence of ester

as a functional group. However, most chemically synthesized artificial esterases only hydrolyze highly activated substrates such as *p*-nitrophenyl esters.<sup>7</sup> Since replacing the *p*-nitrophenyl leaving group with a simple ethyl is able to eliminate the majority of catalysis in some synthetic systems, <sup>27</sup> it is important to develop catalysts for unactivated esters that dominate in natural and man-made products.

We previously reported a molecularly imprinted synthetic esterase capable of hydrolyzing unactivated esters under mild conditions.<sup>23</sup> In molecularly imprinted catalysts, a substrate-resembling template is used to create the imprinted pocket and the catalytic groups are commonly installed through postmodification. In our previous catalyst, the template is a phosphonamidate derivative prepared in multiple-step synthesis and the postmodification is lengthy, making it difficult to scale up the synthesis of the catalyst.

Scheme 1 shows a facile, direct preparation of artificial esterase, with no need for any postmodification. The key lies in the design of the acylthiourea template ( $\mathbf{T}$ ), which resembles both activated substrate  $\mathbf{S1a}$  ( $R = NO_2$ ) and unactivated  $\mathbf{S2}$  in size and shape. Note that the latter is considered an "alkyl ester" because its p-nitrophenyl group is not directly bonded to the acyl. (Its hydrolysis affords a hemiacetal which hydrolyzes spontaneously to release p-nitrophenoxide, which can be monitored by UV-vis spectroscopy at 400 nm.) The thiourea group has



Scheme 1. Preparation of MINP-1 for catalytic hydrolysis of ester S1a for the hydrolysis of S1a.

Two strong hydrogen-bond donors that can interact with 4-vinylben-zoate (1) that contains two hydrogen-bond acceptors. Even though hydrogen bonding interactions are weakened in water by solvent competition, they are strong in the nonpolar microenvironment of the micelle of  $\mathbf{2}$ . In addition, the thiourea sulfur is a good (soft) ligand for the zinc ion in the tridentate complex  $\mathbf{A}$ . Formation of termolecular complex  $\mathbf{1} \cdot \mathbf{T} \cdot \mathbf{A}$  is facilitated also by the higher effective concentrations of the three compounds in the micelle.

With a layer of terminal alkyne groups on the surface, the mixed micelles are readily cross-linked by diazide 3 (step a) and functionalized with monoazide 4 (step b), both via the highly efficient alkyneazide click reaction. UV irradiation of 2,2-dimethoxy-2-phenylacetophenone (DMPA, a photoinitiator) initiates free radical polymerization and cross-linking among the micelle-solubilized divinylbenzene (DVB) and the methacrylates of the surfactants (step c). The termolecular complex 1.T.A is co-polymerized in the same step so that the functional monomers (FMs, i.e., 1 and A) get covalently attached to the micelle core, near the template. Precipitation from acetone and solvent washing afford MINP(A), i.e., the molecularly imprinted nanoparticle (MINP) prepared with complex **A** as the template-binding FM. The template is removed in the meantime. MINP(A') is also prepared without FM 1 and serves as a control catalyst. Another control is the nonimprinted nanoparticle (NINP), prepared without any template and thus having no imprinted pockets. Similarly, catalyst MINP(**B**) is prepared following the same procedures in Scheme 1, using zinc complex **B** to bind the template.

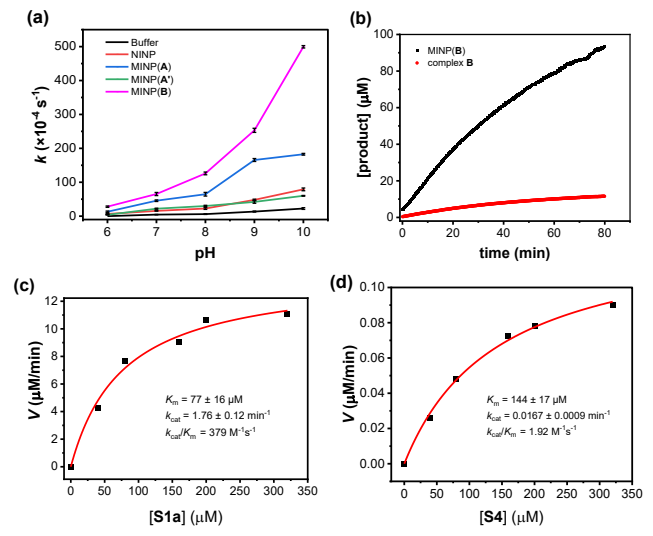
We employed the zinc complexes as the catalytic center because zinc is a common cofactor in natural hydrolases<sup>28,29</sup> and frequently used also in artificial esterases. <sup>14-19</sup> The ligand design in complex  $\bf B$  is inspired by the work of Mareque-Rivas and Williams, who have demonstrated that the *ortho* amino groups work cooperatively with neighboring zinc ions in the hydrolysis of phosphate esters.<sup>30</sup>

Figure 1a shows the pH profiles for the hydrolysis of S1a by MINP(A) and MINP(B), with the control catalysts included for comparison. Over pH 6–10, NINP and MINP(A') display similar activities, with a modest rate acceleration over the background (buffer reaction). MINP(A) and, in particular, MINP(B) exhibit much higher activities, especially at higher pHs. When 500 equivalents of S1a is added to MINP(B), a total turnover number (TON) of 465 is obtained at 80 min (Figure 1b). In contrast, complex B in the same buffer displays very little activity.

MINP(**B**), our best catalyst, resembles enzymes by following Michaelis–Menten kinetics in its hydrolysis of **S1A** (Figure 1c) and, more importantly, unactivated substrate **S2** (Figure 1d). The Michaelis constant ( $K_{\rm M}$ ) for the activated substrate (77  $\mu$ M) is nearly half of that for the unactivated one (144  $\mu$ M). The result is reasonable given the stronger hydrophobicity of **S1a** and the hydrophobically driven substrate binding in water. The catalytic turnover ( $k_{\rm cat}$ ) for **S1a** (1.76 min<sup>-1</sup>) is over 100 times higher than that for **S2** (0.0167 min<sup>-1</sup>). The result is also reasonable.

**S1a** and **S2** are both expected to fit within the active site of MINP(**B**) due to their similarity to the template in size and shape (Scheme 1). Esters **S3** and **S4**, on the other hand, can only fill part of the active site, leaving the rest being filled with water molecules—an unfavorable situation. Indeed, these substrates are significantly less reactive than **S1a** in the presence of MINP(**A**) or MINP(**B**) at pH 9 (Figure 2a) and pH 10 (Figure 2b). Note that at pH 10, MINP(**B**)

is much more active than MINP( $\mathbf{A}$ ) (Figure 1a) and yet is also more selective than MINP( $\mathbf{A}$ ) (Figure 2b). It should be mentioned that p-nitrophenyl acetate ( $\mathbf{S3}$ ) normally hydrolyzes more quickly than the more hydrophobic derivatives under uncatalyzed conditions.



**Figure 1.** (a) pH profile for the hydrolysis of **S1a** under different catalytic conditions at 25 °C. [**S1a**] = 50 μM. [Catalyst] = 10 μM. Buffer: MES for pH 6.0–6.5, HEPES for pH 7.0–8.5, CHES for pH 9.0–10.0. (b) Amount of *p*-nitrophenoxide formed as a function of time in a 25 mM HEPES buffer at 25 °C and pH 7.0, calculated based on an extinction coefficient of  $\epsilon_{400} = 0.0091 \ \mu M^{-1} \ cm^{-1}$ . [**S1a**] = 100 μM. [MINP(**B**)] = complex **B** = 0.2 μM. (c) Michaelis-Menten plot for the hydrolysis of **S1a** by MINP(**B**) in a HEPES buffer at 25 °C and pH 7.0. (d) Michaelis-Menten plot for the hydrolysis of **S2** by MINP(**B**) in a HEPES buffer at 40 °C and pH 7.0. [MINP(**B**)] = 8.0 μM.

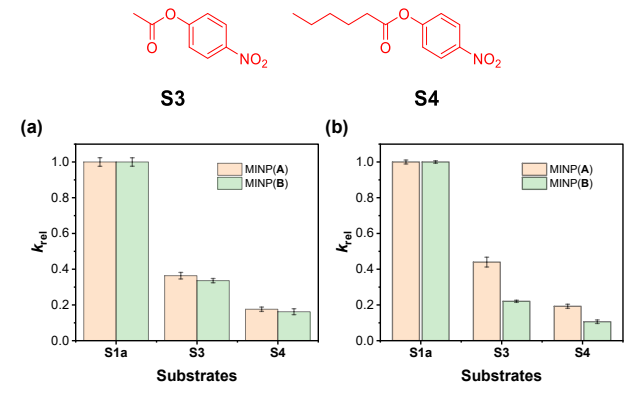


**Figure 2.** Relative rates of hydrolysis of **S1a**, **S3**, and **S4** by the MINP catalysts at pH 9 (a) and pH 10 (b) at  $25 \,^{\circ}$ C, respectively. [substrate] =  $50 \,\mu\text{M}$ . [Catalyst] =  $10 \,\mu\text{M}$ .

To understand the mechanism for the catalysis, we studied the hydrolyses of a series of *para*-substituted ester substrates (**S1a-f**) by MINP(**B**). The resulting Hammett plot gives a reaction constant ( $\rho$ ) of 1.52 in pH 7.0 HEPES buffer (Figure 3). In the hydrolysis of aryl esters, the amount of negative charge on the phenol oxygen is strongly affected by the nucleophiles involved.<sup>31,32</sup> A  $\rho$  value of 1–1.2 is typically observed for strong, anionic oxygen-based nucleophiles such as hydroxide, whereas  $\rho$  = 0.5–0.7 is common for general based-catalyzed nucleophilic attack by water, due to a smaller amount of negative charge build up on the phenol oxygen in the latter case. If

these numbers obtained from solution reactions can be used to understand the mechanistic picture inside the MINP, a  $\rho$  value of 1.52 indicates a substantial negative charge buildup on the phenol oxygen, possibly from a strong negatively charged oxygen nucleophile (e.g., a metal-bound hydroxide and/or the active site carboxylate).

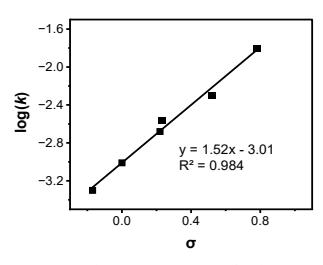


**Figure 3.** Hammett σ–ρ correlation in the hydrolysis of *para*-substituted **S1a–f** catalyzed by MINP(**B**). Reaction rates were measured in 25 mM 3HEPES buffer (pH 7.0) at 25 °C. [ester] = 50 μM. [MINP(**B**)] = 10 μM. σ values: p-NO<sub>2</sub>, 0.78; p-CH<sub>3</sub>CO, 0.52; p-Cl, 0.23; p-CHO, 0.22; p-H, 0.00; p-CH3, -0.17.

A general base catalysis involves a cleavage of water O–H bond in the rate-limiting step and affords a primary solvent isotope effect significantly larger than 1.<sup>33-36</sup> Instead, both MINP(**A**) and MINP(**B**) give a  $k_{\rm H2O}/k_{\rm D2O}$  value of ca. 1.1 (Table 1), indicating no O–H bond cleavage in the transition state.

**Table 1.** Pseudo-first-order rate constants and solvent kinetic isotope effects of hydrolysis of **S1a** catalyzed by MINPs at 25 °C.<sup>a</sup>

entry	catalyst	solvent	k (×10 <sup>-4</sup> s <sup>-1</sup> )	$k_{ m H2O}/k_{ m D2O}$
1	MINP(A)	H <sub>2</sub> O	$47 \pm 2.0$	1.14
2	MINP(A)	$D_2O$	$41\pm1.0$	
3	MINP(B)	$H_2O$	$56 \pm 0.5$	1.12
4	MINP(B)	$D_2O$	$50 \pm 1.5$	

<sup>a</sup> Reaction rates were measured by monitoring the appearance of 4-nitrophenolate at 400 nm in MES buffer. [MINP] = 10 μM. [**S1A**] = 50 μM. Because water and  $D_2O$  have different dissociation constants, the pD value was determined by adding 0.4 to the pH meter reading.<sup>34</sup>

We included 4-vinylbenzoate (1) as one of the FMs because we had hypothesized that, after polymerization into the micelle core, its carboxylic acid could act as a general acid to help the departure of the leaving group. The pH profiles in Figure 1a do not support such a picture, as the highest rate acceleration occurs at pH 9-10, at which the carboxylic acid should be deprotonated. Nonetheless, FM 1 is clearly helpful to the catalysis, since  $MINP(\mathbf{A}')$  without the acid is consistently underperforms MINP(A) at all pHs tested (Figure 1a)—the same is true for MINP(**B**) (data not shown). It is not entirely clear to us how a carboxylate can help the hydrolysis. One possibility is that it stabilizes the metal-bound hydroxide by hydrogen bonds, essentially facilitating the deprotonation of the zinc-bound water to generate the active-site nucleophile. This is similar to the role of ortho-amino groups proposed by Mareque-Rivas and Williams in their catalyst.<sup>30</sup> Another possibility is that the active site carboxylate acts a nucleophilic catalyst, as in some carboxypeptidases.<sup>37</sup>

Micellar imprinting has remarkable abilities to reproduce structural features of the template in the imprinted site as a result of a nanoconfinement effect.<sup>38</sup> MINPs easily distinguish the addition,<sup>38</sup> removal,<sup>38</sup> and shift<sup>39</sup> of a single methyl (or methylene) group in the

guest. However, converting these nanoparticles into catalysts often involves lengthy postmodification. This work demonstrates a direct synthesis of ester-hydrolyzing catalysts, with the entire synthesis/purification complete in less than 2 days once the template, surfactant, FMs, and cross-linkers are available. Importantly, the resulting artificial esterase differentiates substrates based on their size, shape, and hydrophobicity. Ester as a functional group is prevalent in both small molecules and polymers. Catalysts capable of hydrolyzing unactivated esters with substrate-selectivity may open up new ways to process ester-containing molecules and polymers with precision.

# **ASSOCIATED CONTENT**

### **Data Availability Statement**

The data underlying this study are available in the published article and its Supporting Information.

# **Supporting Information**

Experimental details, characterization of the catalysts, additional data, and NMR and MS spectra for the new compounds synthesized. This material is available free of charge via the Internet at http://pubs.acs.org.

# **AUTHOR INFORMATION**

# **Corresponding Author**

Yan Zhao - http://orcid.org/0000-0003-1215-2565; E-mail: zhaoy@iastate.edu\*

#### **Author**

Mohan Lakavathu - Department of Chemistry, Iowa State University, Ames, Iowa 50011-3111, U.S.A.

#### **Notes**

The authors declare no competing interests.

# **ACKNOWLEDGMENT**

We thank NSF (CHE-2246635) for supporting the research.

#### **REFERENCES**

- (1) Kirsch, J. F.; Jencks, W. P. Nonlinear Structure-Reactivity Correlations. The Imidazole-Catalyzed Hydrolysis of Esters. *J. Am. Chem. Soc.* **1964**, *86*, 837-846.
- (2) Quinn, D. M. Acetylcholinesterase: enzyme structure, reaction dynamics, and virtual transition states. *Chem. Rev.* **1987**, *87*, 955-979.
- (3) Berg, O. G.; Gelb, M. H.; Tsai, M. D.; Jain, M. K. Interfacial enzymology: the secreted phospholipase A<sub>2</sub>-paradigm. *Chem. Rev.* **2001**, *101*, 2613-2654.
- (4) Trainor, G. L.; Breslow, R. High acylation rates and enantioselectivity with cyclodextrin complexes of rigid substrates. *J. Am. Chem. Soc.* **1981**, *103*, 154-158.
- (5) Cram, D. J.; Katz, H. E.; Dicker, I. B. Host-guest complexation. 31. A transacylase partial mimic. *J. Am. Chem. Soc.* **1984**, *106*, 4987-5000.
- (6) Breslow, R.; Dong, S. D. Biomimetic Reactions Catalyzed by Cyclodextrins and Their Derivatives. *Chem. Rev.* **1998**, 98, 1997-2012.
- (7) Nothling, M. D.; Xiao, Z.; Bhaskaran, A.; Blyth, M. T.; Bennett, C. W.; Coote, M. L.; Connal, L. A. Synthetic Catalysts Inspired by Hydrolytic Enzymes. *ACS Catal.* **2019**, *9*, 168-187.
- (8) Wulff, G.; Liu, J. Design of biomimetic catalysts by molecular imprinting in synthetic polymers: the role of transition state stabilization. *Acc. Chem. Res.* **2012**, 45, 239-247.
- (9) Liu, J.-q.; Wulff, G. Functional Mimicry of Carboxypeptidase A by a Combination of Transition State Stabilization and a Defined Orientation of Catalytic Moieties in Molecularly Imprinted Polymers. *J. Am. Chem. Soc.* **2008**, 130, 8044-8054.
- (10) Robinson, D. K.; Mosbach, K. Molecular imprinting of a transition state analogue leads to a polymer exhibiting esterolytic activity. *J. Chem. Soc., Chem. Commun.* **1989**, 969-970.

- (11) Ohkubo, K.; Urata, Y.; Hirota, S.; Honda, Y.; Fujishita, Y.-i.; Sagawa, T. Homogeneous esterolytic catalysis of a polymer prepared by molecular imprinting of a transition state analogue. *J. Mol. Catal.* **1994**, *93*, 189-193.
- (12) Sellergren, B.; Karmalkar, R. N.; Shea, K. J. Enantioselective Ester Hydrolysis Catalyzed by Imprinted Polymers. 2. J. Org. Chem. 2000, 65, 4009-4027.
- (13) Arifuzzaman, M.; Zhao, Y. Artificial Zinc Enzymes with Fine-Tuned Catalytic Active Sites for Highly Selective Hydrolysis of Activated Esters. *ACS Catal.* **2018**, *8*, 8154-8161.
- (14) Zastrow, M. L.; Peacock, A. F. A.; Stuckey, J. A.; Pecoraro, V. L. Hydrolytic catalysis and structural stabilization in a designed metalloprotein. *Nat. Chem.* **2012**, *4*, 118-123.
- (15) Zastrow, M. L.; Pecoraro, V. L. Influence of Active Site Location on Catalytic Activity in de Novo-Designed Zinc Metalloenzymes. *J. Am. Chem. Soc.* **2013**, *135*, 5895-5903.
- (16) Rufo, C. M.; Moroz, Y. S.; Moroz, O. V.; Stohr, J.; Smith, T. A.; Hu, X. Z.; DeGrado, W. F.; Korendovych, I. V. Short peptides self-assemble to produce catalytic amyloids. *Nat. Chem.* **2014**, *6*, 303-309.
- (17) Song, W. J.; Tezcan, F. A. A designed supramolecular protein assembly with in vivo enzymatic activity. *Science* **2014**, 346, 1525-1528.
- (18) Burton, A. J.; Thomson, A. R.; Dawson, W. M.; Brady, R. L.; Woolfson, D. N. Installing hydrolytic activity into a completely de novo protein framework. *Nat. Chem.* **2016**, *8*, 837-844.
- (19) Studer, S.; Hansen, D. A.; Pianowski, Z. L.; Mittl, P. R. E.; Debon, A.; Guffy, S. L.; Der, B. S.; Kuhlman, B.; Hilvert, D. Evolution of a highly active and enantiospecific metalloenzyme from short peptides. *Science* **2018**, *362*, 1285-1288.
- (20) Nothling, M. D.; Xiao, Z.; Hill, N. S.; Blyth, M. T.; Bhaskaran, A.; Sani, M.-A.; Espinosa-Gomez, A.; Ngov, K.; White, J.; Buscher, T.; Separovic, F.; O'Mara, M. L.; Coote, M. L.; Connal, L. A. A multifunctional surfactant catalyst inspired by hydrolases. *Sci. Adv.* **2020**, *6*, eaaz0404.
- (21) Makhlynets, O. V.; Korendovych, I. V. A single amino acid enzyme. *Nat. Catal.* **2019**, 2, 949-950.
- (22) Lee, Y.; Devaraj, N. K. Lipase mimetic cyclodextrins. Chem. Sci. 2020, 12, 1090-1094
- (23) Arifuzzaman, M. D.; Bose, I.; Bahrami, F.; Zhao, Y. Imprinted polymeric nanoparticles as artificial enzymes for ester hydrolysis at room temperature and pH 7. *Chem Catal.* **2022**, *2*, 2049-2065.
- (24) Yoshida, S.; Hiraga, K.; Takehana, T.; Taniguchi, I.; Yamaji, H.; Maeda, Y.; Toyohara, K.; Miyamoto, K.; Kimura, Y.; Oda, K. A bacterium that degrades and assimilates poly(ethylene terephthalate). *Science* **2016**, *351*, 1196-1199.
- (25) Tournier, V.; Topham, C. M.; Gilles, A.; David, B.; Folgoas, C.; Moya-Leclair, E.; Kamionka, E.; Desrousseaux, M. L.; Texier, H.; Gavalda, S.; Cot, M.; Guémard, E.; Dalibey, M.; Nomme, J.; Cioci, G.; Barbe, S.; Chateau, M.; André,

- I.; Duquesne, S.; Marty, A. An engineered PET depolymerase to break down and recycle plastic bottles. *Nature* **2020**, *580*, 216-219.
- (26) Lu, H.; Diaz, D. J.; Czarnecki, N. J.; Zhu, C.; Kim, W.; Shroff, R.; Acosta, D. J.; Alexander, B. R.; Cole, H. O.; Zhang, Y.; Lynd, N. A.; Ellington, A. D.; Alper, H. S. Machine learning-aided engineering of hydrolases for PET depolymerization. *Nature* **2022**, *604*, *662-667*.
- (27) Menger, F. M.; Ladika, M. Origin of rate accelerations in an enzyme model: the p-nitrophenyl ester syndrome. *J. Am. Chem. Soc.* **1987**, *109*, 3145-3146.
- (28) Vallee, B. L.; Auld, D. S. Zinc coordination, function, and structure of zinc enzymes and other proteins. *Biochemistry* **1990**, *29*, 5647-5659.
- (29) Coleman, J. E. Zinc enzymes. Curr. Opin. Chem. Biol. 1998, 2, 222-234.
- (30) Feng, G.; Natale, D.; Prabaharan, R.; Mareque-Rivas, J. C.; Williams, N. H. Efficient Phosphodiester Binding and Cleavage by a Zn<sup>II</sup> Complex Combining Hydrogen-Bonding Interactions and Double Lewis Acid Activation. *Angew. Chem. Int. Ed.* **2006**, *45*, 7056-7059.
- (31) Bruice, T. C.; Benkovic, S. J. The Compensation in  $\Delta H^{\dagger}$  and  $\Delta S^{\dagger}$  Accompanying the Conversion of Lower Order Nucleophilic Displacement Reactions to Higher Order Catalytic Processes. The Temperature Dependence of the Hydrazinolysis and Imidazole-Catalyzed Hydrolysis of Substituted Phenyl Acetates. *J. Am. Chem. Soc.* **1964**, *86*, 418-426.
- (32) Kirsch, J. F.; Clewell, W.; Simon, A. Multiple structure reactivity correlations. Alkaline hydrolyses of acyl and aryl-substituted phenyl benzoates. *J. Org. Chem.* **1968**, 33, 127-132.
- (33) Bender, M. L.; Pollock, E. J.; Neveu, M. C. Deuterium Oxide Solvent Isotope Effects in the Nucleophilic Reactions of Phenyl Esters. *J. Am. Chem. Soc.* **1962**, *84*, 595-599.
- (34) Gibbs, R. A.; Benkovic, P. A.; Janda, K. D.; Lerner, R. A.; Benkovic, S. J. Substituent effects of an antibody-catalyzed hydrolysis of phenyl esters: further evidence for an acyl-antibody intermediate. *J. Am. Chem. Soc.* **1992**, *114*, 3528-3534
- (35) Jencks, W. P.; Carriuolo, J. General Base Catalysis of Ester Hydrolysis 1. J. Am. Chem. Soc. 1961, 83, 1743-1750.
- (36) Stefanidis, D.; Jencks, W. P. General Base Catalysis of Ester Hydrolysis. *J. Am. Chem. Soc.* **1993**, *115*, 6045-6050.
- (37) Christianson, D. W.; Lipscomb, W. N. Carboxypeptidase A. Acc. Chem. Res. 1989, 22, 62-69.
- (38) Chen, K.; Zhao, Y. Effects of nano-confinement and conformational mobility on molecular imprinting of cross-linked micelles. *Org. Biomol. Chem.* **2019**, *17*, 8611-8617.
- (39) Awino, J. K.; Gunasekara, R. W.; Zhao, Y. Sequence-Selective Binding of Oligopeptides in Water through Hydrophobic Coding. *J. Am. Chem. Soc.* **2017**, 139, 2188-2191.

